Journal of the Indian Society of Remote Sensing (June 2024) 52(6):1201–1222
https://doi.org/10.1007/s12524-024-01872-8

RESEARCH ARTICLE

Identifying Groundwater Potential Regions in Sokoto Basin, Northwestern Nigeria: An Integrated Remote Sensing, GIS, and MIF Techniques

Ernest O. Akudo[1] · **Stanley I. Ifediegwu**[2] · **Jamilu B. Ahmed II**[1] · **Godwin O. Aigbadon**[1]

Received: 12 January 2022 / Accepted: 12 April 2024 / Published online: 15 May 2024

Abstract

Sokoto basin is known to experience an acute shortage of surface and groundwater resources due to climate change, increasing aridity, and land degradation among several other concerns. Being in an agrarian environment, the people are faced with the hardship of a limited supply of water, especially for dry season crop cultivation. Therefore, this study aims to identify and delineate good groundwater potential zones to guide its exploitation. The study utilized nine GWPR factors, including geology, soil property, geomorphology, slope, lineament density, drainage density, rainfall, land use/land cover, and groundwater level fluctuation. These factors were sourced from remotely sensed data and reliable archived hydrological data, after which thematic layers were prepared and assembled in the ArcGIS 10.5 environment. The Multi-Influence Factor (MIF) analysis techniques and the weighted overlay method were used to assign weights and the groundwater potential map of the study area was generated. The results classified the basin into, poor, moderate, good, and very good groundwater potential regions, with the spatial expanse of 17.4 km^2 (0.028%), 34,470.6 km^2 (54.8%), 26,380.2 km^2 (42.0%), and 2020.5 km^2 (3.2%), respectively. The good to very good potential regions are mostly domiciled in the southern part of the basin covering most parts of Kebbi State. In contrast, the moderate to the poor regions are restricted to the northern part of the basin essentially covering most parts of Sokoto and Zamfara States. Validation shows that the results are in tandem with the outcome of the GIS and MIF techniques.

Keywords Groundwater potential regions · Geographic information system · Multi influence factor · Sokoto Basin

Introduction

The significance of water, specifically freshwater, has undoubtedly been identified with the origin of man. Freshwater constitutes less than three percent of the water resources of the world, yet it remains one of the most important renewable resources provided by nature and serves as support and succor to all terrestrial ecosystems (Odada, 2006). Over 96% of the global supply of water, accounting for approximately 332.5 million cubic meters is saline water. Additionally, of the meager fresh water available for our use, over 68% of it exists in ice and glacial states. Another 30% of the remaining freshwater exists in the subsurface as groundwater (Igor, 1993). Groundwater remains a high priority compared to surface water because it is found in a relatively safer and cleaner state and is often of better quality before treatment (Akudo et al., 2010). The occurrence of groundwater determines the location of settlements and the trend of civilizations, as humans need this resource for domestic, agricultural, and other uses (Gupta & Srivastava, 2010; Ostad-Ali-Askari et al., 2017). In Nigeria alone, about three-quarters of the population depends on groundwater for domestic purposes (Goni, 2006), and more than half of the available freshwater is somewhat assigned already (Musa, 1997), meaning that there are deficiencies in the quantity of available freshwater with increasing population. Published evidence shows that Nigeria's freshwater need may increase from 50×10^9 l/year (Akujieze et al., 2003) to 224×10^9 l/year (Hanidu, 1990) with increasing population in the coming years. UNEP (2002) report indicates that about 33% of

✉ Ernest O. Akudo
ernest.akudo@fulokoja.edu.ng

[1] Department of Geology, Faculty of Sciences, Federal University, Lokoja, Kogi State, Nigeria

[2] Department of Geology, Faculty of Physical Sciences, University of Nigeria, Nsukka, Nigeria

the world's population live in countries with problems of mild to acute water scarcity, with the problems taking their toll more on the poor (FAO, 1995).

In the Sokoto basin, an assessment of water demand and availability under varying scenarios of temperature, rainfall, and evapotranspiration (Abdullahi et al., 2014) shows that the basin will soon experience a shortage of both surface and groundwater, especially because of climate change, increasing aridity, desertification, land degradation, construction of several unplanned boreholes for irrigation, low precipitation, lowering of the water table, amongst other challenges (Adelana et al., 2003; Ostad-Ali-Askari & Shayannejad, 2021)). The majority of the already published research in the Sokoto basin relied on conventional methods, such as geological, hydrogeological, and geophysical methods deployed for subsurface investigation and siting of boreholes (Akinbiyi et al., 2019; Musa & Mohammed, 2015; Abdullahi et al., 2014; Adamu, 2019; Hamidu et al., 2016). As good as these methods seem, the major disadvantages range from being cumbersome to expensive, and requiring a lot of time to deploy.

Currently, RS and GIS techniques are being deployed by many researchers for the identification of groundwater potential zones. These techniques include the weighed overlay method (WOM) (Walker & Nilkawar, 2014; Abdullahi et al., 2013; Kaliraj et al., 2015), multi-influence factor analysis (Raju et al., 2019; Das and Paradeshi, 2018; Al-Abadi et al., 2017), frequency ratio model (FRM) (Manap et al., 2013; Oh et al., 2011), random forest (RF) (Ahmed II & Pradhan, 2019), analytical hierarchy procedure (AHP) (Allafta et al., 2020; Ogbonnaya et al., 2020; Ifediegwu et al., 2019; Lakeshmi & Reddy, 2018; Ifediegwu, 2022), etc. Out of all these techniques, the multi-influence factor analysis is the most reliable and achievable with minimal cost (Raju et al., 2019). Few studies have explored remote sensing and GIS technology in groundwater potential studies in the Sokoto basin. Abdullahi et al. (2013) utilized the weighted overlay method (WOM), while Kudamnya et al. (2017) deployed the analytical hierarchy process (AHP). These techniques, although robust, have some elements of subjectivity compared to the more robust multi-influence factor analysis (MIF), which analyses the interrelationship between all factors and categorizes the relationship into major and minor basis before assigning weightage to a factor. For this important reason, the MIF technique was utilized for the first time in the Sokoto basin.

Freshwater demand in the study area stands at over 16 billion cubic meters per month (Abdullahi et al., 2014) with only a paltry 10% of this water available as the supply for drinking, agricultural practices, industrial use, livestock needs, and irrigation purposes. Cases of failure of boreholes due to low yields (Hamidu et al., 2016; Maduabuchi, 2004) and a decline in the water table have also been reported in parts of Sokoto state which is part of the study area (Umar, 2000). Surface water supply schemes that were meant to complement groundwater sources are in a comatose state, leaving groundwater as the only source of supply required to meet the already highlighted freshwater needs. This research was therefore implemented using the most recent geospatial techniques to identify groundwater potential regions in the study area.

Study Area

The Sokoto basin situated at latitudes 11° 0′ 0″ N–14° 0′ 0″ N and a longitude of 3° 0′ 0″ E–6° 0′ 0″ E, makes up a portion of the sub-basins of the Illumedan basin of West Africa (Fig. 1) and has a spatial extent of 62,888.66 sq. km, with an elevation of approximately 131–845 m above mean sea level (Abdullahi et al., 2014). It comprises parts of Sokoto, Zamfara, and the Kebbi States, and it shares borders with the Niger Republic and the Northern part of the Benin Republic.

The mean monthly rainfall collated for ten years (2002–2011) showed very low values, with rainfall concentrated between April and October each year (Fig. 2). Records of average annual rainfall are also low (470 mm) with most rainfall events confined to May to September, with October to April recording little or no rainfall in years. Ranges of evaporation (80–210 mm) and temperature (24–38 °C) are high, making most months of the year hot and dry except December to January, which experiences low values (Adelana et al., 2003). The relative humidity is low most of the year with remarkable increases between June and September, which is the wet season.

The vegetation is defined by stunted and thorny shrubs, usually acacia species. The entire basin can be said to be of Sudan and Sahel Savanna and classified as semi-arid. Ekpoh and Ekpenyong (2011) described the basin as having landforms prone to flooding, with the flood events providing rich soils that support agricultural practices.

The hydrology of the basin indicates that drainage is controlled by the river Sokoto, which is a very important component of the Niger River drainage system. The Sokoto river originates from the 600 to 900 m high Mashika and Dunia highland areas adjoining the basin on the eastern flank together with its major tributaries, the Ka, Zamfara, and Rima, and descends rather sluggishly down a gentle gradient toward the northwest, where around Sokoto town, it merges with the Rima River in the north, diverting to a southward flow, picking up the Zamfara and Ka before moving downwards to the river Niger. The Sokoto river system is seasonal in the eastern part where it originates. However, in the western part of the river system, it is recharged substantially by groundwater flow making it perennial (Abdullahi et al., 2014).

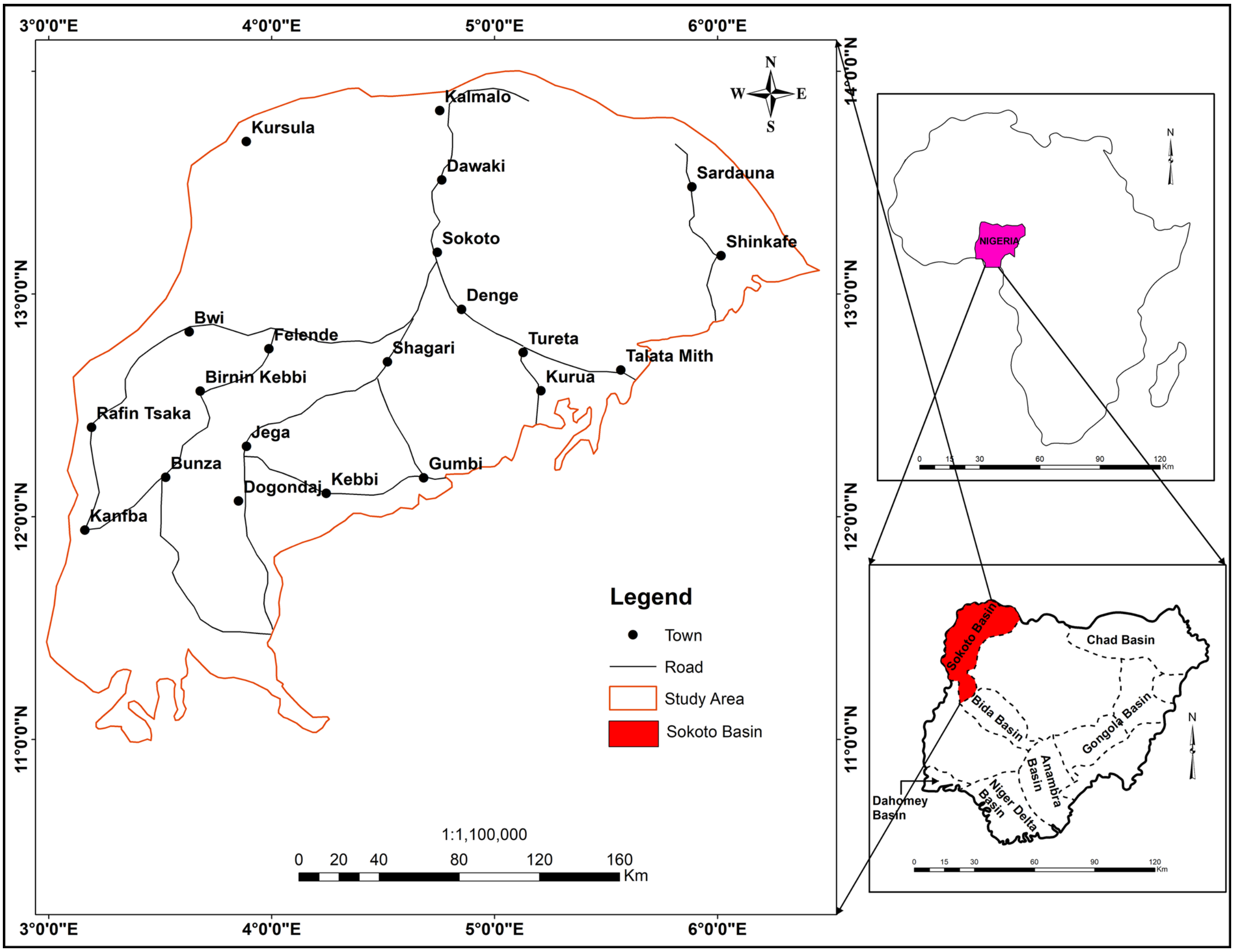

Fig. 1 Location map of the Sokoto Basin, Northwestern Nigeria. (Insert: Map of Nigeria and Africa)

The hydrogeology of the study area is defined by five aquifer units, namely Gwandu, Kalambaina, Wurno, Taloka, and Gundumi/Illo Formation respectively. The confining layers (aquicludes) are Gamba, Dange, and Dukamaje Formations respectively. The Kalambaina Formations (Sokoto Group) are made of limestones with cavities and joints, and have layers with good aquifer characteristics to provide water (Hamidu et al., 2016). The Gundumi/Illo Formation comprises coarse sand and gravels. It is unconformably underlain by the Basement Complex and occurs only in Zamfara States (Northwestern part of the basin), making both the most limited in terms of area extent. Dange Formations, Dukamaje Formations, and Gamba Formations (largely shale, siltstone, and clay) serve as confining layers (Oteze, 1976). The Wurno/Taloka Formation (Maastrichtian in age) are parts of the Rima Group and have similar geology, consisting of fine-medium sands. The Wurno Formation overlies the Dukamaje and Taloka, and both Formations are the most widespread in terms of lateral extent, occurring in all three states (Sokoto, Kebbi, and Zamfara) that make up the basin. The Gwandu Formation, which overlies the rest, is the youngest (Eocene-Miocene) of all the Formations, and it consists of medium to coarse sands. It laterally extends across Sokoto and Kebbi States and serves as aquifer material in those parts of the basin.

Materials and Methods

Data Acquisition

Remote Sensing Data

Remote sensing data, including Landsat OLI/TIRS and the Digital Elevation Model (DEM) from the Shuttle Radar Topographic Mission (SRTM), all of 30 m spatial resolution were obtained from the US Geological Survey (USGS) website (https://earthexplorer.usgs.gov). These data

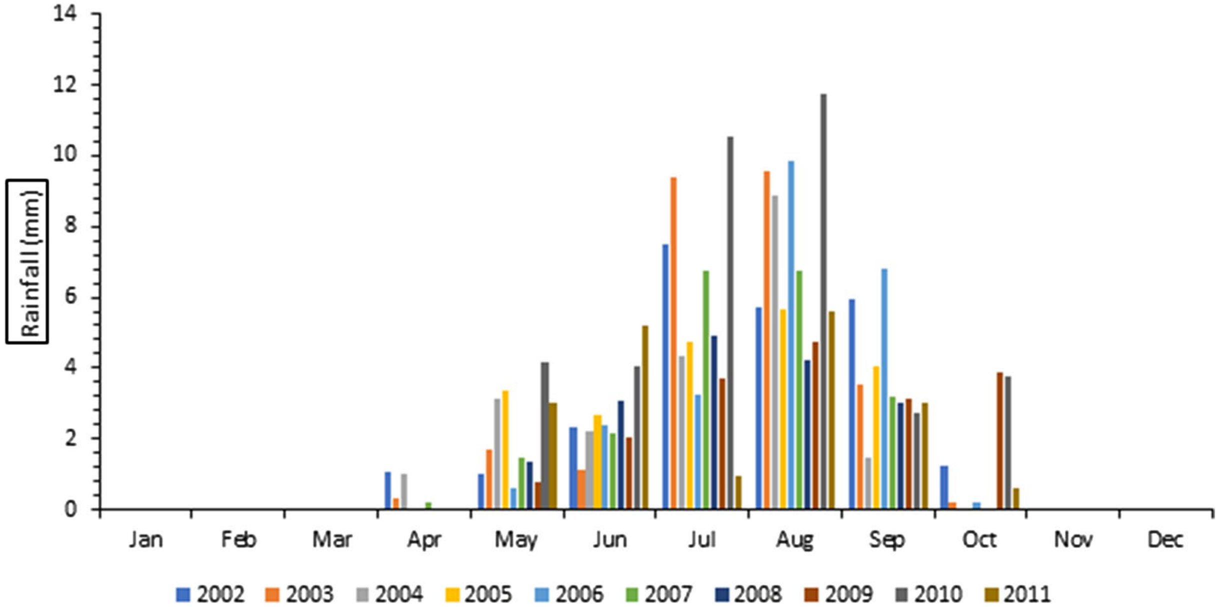

Fig. 2 Mean monthly rainfall records for 10 years (2002–2011) in the study area. (*Source*: NIMET)

collected in December 2020 were employed to obtain the drainage density, slope, and land use/ land cover thematic layers.

Well Data

Data from 45 boreholes, including borehole depth, aquifer type, thickness, geologic materials making up the aquifers, borehole yields, as well as wet and dry season static water levels, were obtained from the Sokoto State Water Corporation (Table 1). This dataset serves two purposes: first, the preparation of groundwater level fluctuation thematic layer using the change in static water levels, and second, MIF model validation using the borehole yield data.

Rainfall Data

The yearly average rainfall data for ten years from 2002 to 2011 were collected from ten different stations of the Nigerian Meteorological Agency (NIMET) located within the basin (Fig. 2). The data contain the coordinates of each recording station, together with the daily record of rainfall, and followed by the monthly to the yearly average.

Other Datasets

Conventional data, viz; analog soil, geology, and geomorphology maps, were gathered from the Food and Agriculture Organization (FAO) and the Nigerian Geological Survey Agency (NGSA), respectively. These were then processed, georeferenced (WGS, 1984), projected (UTM Zone 32° N), and converted to raster format in the ArcGIS 10.5 environment.

Preparation of Thematic Layers

As stated earlier, nine (9) factors were selected for modeling the groundwater potential of the study area (Fig. 3) based on the literature review and, of course, data availability. The methods employed for preparing the nine (9) factors into thematic layers are discussed below.

Geology (GE), Geomorphology (GM), and Soil Property (SP)

Geology is said to be one of the main initiators of the hydrologic processes (Miller et al., 1990), thus controlling the way aquifers are recharged. Geomorphology is defined by the geology of an area, and it provides clues for groundwater occurrence depending largely on the landforms observed (Waiker & Nilawar, 2014). The soil, on the other hand, is a product of rock weathering, and according to Das (2017), it serves as a very influential factor in regards to the rate and amount of water infiltration, especially from precipitation to the subsurface to recharge aquifers. Porosity, permeability, texture, etc., can either inhibit or enhance the chances of water reaching the subsurface through pores to saturate aquifers. Thematic layers of geology, geomorphology, and soil were prepared from existing maps on a scale of 1: 100,000 obtained from

Table 1 Borehole yield data from study area

Well no	Latitude (^{0}N)	Longitude (^{0}E)	Well depth (m)	Aquifer type	Aquifer thickness (m)	Material	Yield (l/s)	SWL (m)	Classification
1	4.663592	13.828252	48	Unconfined	4.9	Limestone	1.67	32.0	Poor
2	5.845819	13.495129	50	Unconfined	6.1	Limestone	0.4	46.5	Poor
3	5.522691	13.388148	48	Unconfine	4.7	Limestone	0.17	40.0	Poor
4	5.234168	13.431765	49	Unconfined	5.3	Limestone	1.1	45.8	Poor
5	4.892306	13.311843	45	Unconfined	4.5	limestone	0.47	40.8	Poor
6	5.35745	13.42631	50	Unconfined	4.6	Limestone	0.47	37.0	Poor
7	5.37853	13.43888	45	Unconfined	6.1	Limestone	2.25	40.2	Moderate
8	5.37769	13.44052	44	Unconfined	4.5	Limestone	0.35	39.0	Poor
9	5.15223	12.59515	50	Unconfined	5.0	Limestone	0.6	38.5	Poor
10	4.98164	12.59951	38	Unconfined	5.3	Fine-medium sand	6.25	17	Very good
11	4.6391	12.66271	55	Unconfined	6.0	Fine-medium sand	6.67	42	Very good
12	4.62757	12.66277	57	Unconfined	6.3	Fine-medium sand	6.67	37	Very good
13	4.127155	12.699731	65	Unconfined	7.3	Medium sands	2.97	34	Moderate
14	3.705465	12.834635	60	Unconfined	3.8	Medium sands	2.5	37	Moderate
15	4.190262	12.074831	66	Unconfined	3.5	Medium sands	2.75	44.7	Moderate
16	3.972324	12.228927	55	Unconfined	4.6	Medium sands	3.3	35	Moderate
17	6.256876	13.152215	40	Confined	3.5		2.28	45.8	Moderate
18	4.552549	12.298006	36	Confined	3.3	Medium sands	2.58	8	Moderate
19	5.276788	12.580485	35	Unconfined	12.0	Coarse sand	3.2	12	Moderate
20	3.927617	13.660937	36	Unconfined	7.3	Medium sands	4.0	18	Moderate
21	4.192260	13.687089	43.2	Unconfined	10.1	Medium sands	3.08	43.2	Moderate
22	4.795781	13.005954	76	Unconfined	4.1	Limestone	3.5	31.6	Moderate
23	5.740137	13.183802	75	Confined	7.1	Medium sands	5.2	22	Good
24	5.606692	12.686399	80	Unconfined	7.7	Fine -medium sand	4.95	53	Good
25	4.034604	12.429164	54.5	Unconfined	11.2	Medium sands	5.42	36.4	Good
26	3.793952	12.842963	85	Unconfined	10	Medium sands	4.2	38	Good
27	4.442324	12.323027	60	Unconfined	4.7	Fine sand	2.2	47	Moderate
28	3.164366	11.822272	63.2	Unconfined	10.7	Medium sands	4.2	48.3	Good
29	3.205363	11.804063	66	Unconfined	11.2	Medium sands	5.0	36.2	Good
30	3.491585	12.187172	54.5	Unconfined	6.4	Fine sands	3.08	12.8	Moderate
31	3.512061	12.321010	63.1	Unconfined	8.6	Medium sands	5.53	22	Good
32	5.179985	12.517873	30	Unconfined	6	Coarse sands	4.5	9.1	Good
33	5.067061	12.512662	47	Unconfined	7.4	Medium sands	4.7	22	Good
34	4.727496	12.102950	55	Unconfined	6.3	Fine sands	4.0	33	Moderate
35	4.480892	12.693120	35.3	Unconfined	7.8	Coarse sands	5.3	10.2	Good
36	4.633587	12.717157	43	Unconfined	5.6	Medium sands	4.2	25	Moderate
37	4.866401	13.193509	72	Unconfined	10.4	Limestones	6.25	42	Very good
38	6.036409	13.117744	62	Unconfined	82	Medium sands	5.67	27.4	Good
39	3.901789	11.281281	38	Unconfined	11.3	Coarse sands	6.7	28.9	Very good
40	3.713929	11.449589	45	Unconfined	9.2	Coarse sands	6.67	23	Very good
41	3.690538	11.728011	37	Unconfined	10.7	Coarse sands	7.0	25.4	Very good
42	3.739498	12.379605	65	Unconfined	7.8	Medium-coarse sands	6.67	21.8	Very good
43	3.798804	11.758610	57	Unconfined	6	Medium sands	5.35	19.7	Good
44	3.969866	11.929777	42	Unconfined	10.2	Coarse sands	6.2	25	Very good
45	3.809077	12.538270	55.4	Unconfined	5.8	Medium sands	4.1	29	Good

Note: 0-2 l/s (Poor yield), 2.1–4.0 l/s (Moderate yield), 4.1–6.0 l/s (Good yield), and > 6 l/s (Very good)

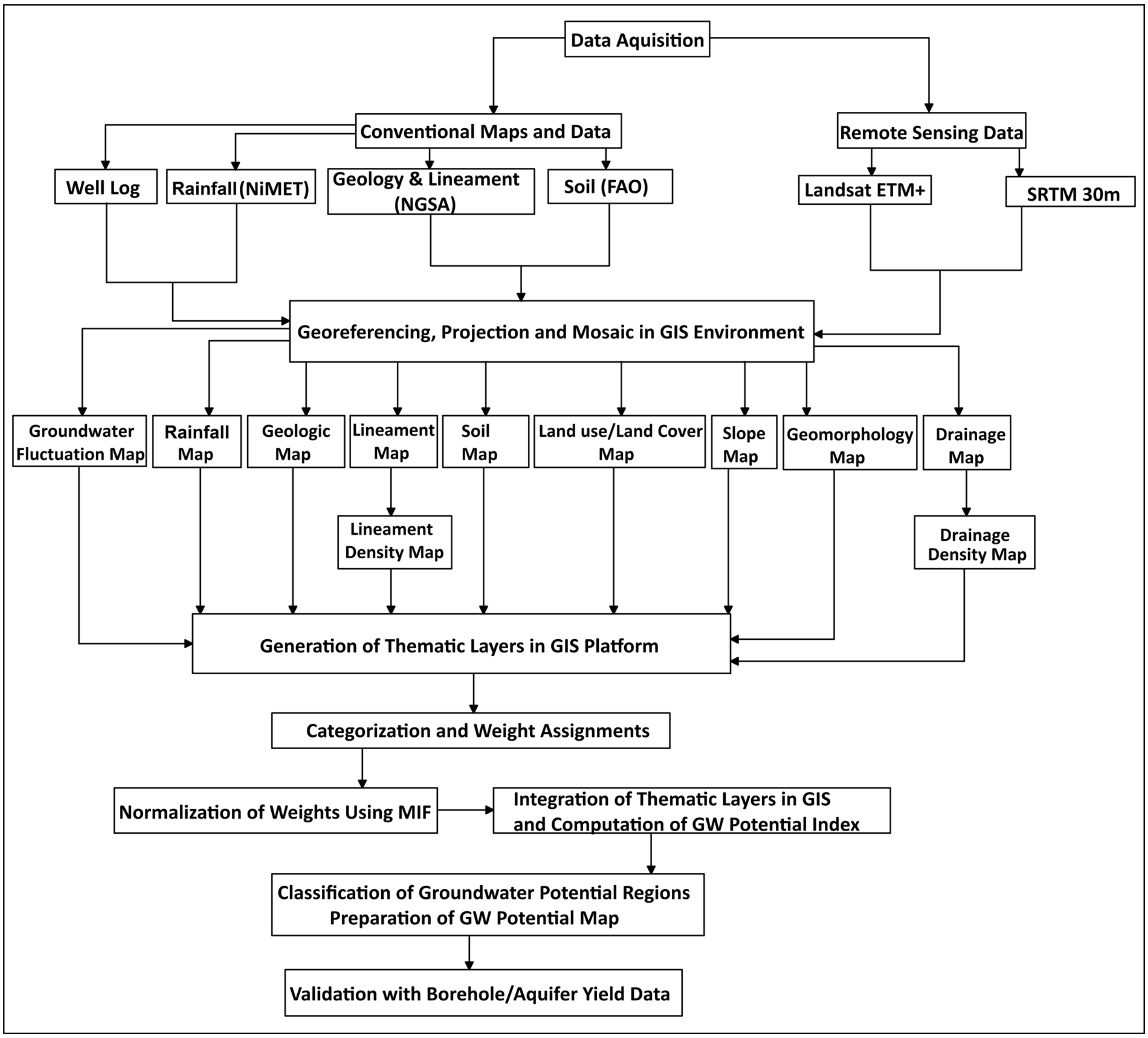

Fig. 3 Flow chart of methodology for characterizing groundwater potential regions in the study area, applying RS, GIS, and MIF techniques

NGSA and FAO, respectively. These were scanned and fed into the ArcGIS 10.5 computing environment and further georeferenced, digitized, and classified according to their potential for groundwater (Fig. 3).

Drainage density (DD), Lineament Density (LD), Slope (SL), and Land Use/Land Cover (LULC)

Drainage is an expression of surface water channels and interconnectivity. Drainage density is related to slope and surface runoff, in the sense that an area with high drainage density usually has a high slope (steep slope) and high surface runoff. Such areas with high slope density always have low water infiltration rates because the fast water movement decreases the retention time required for better infiltration to occur (Guru et al., 2017). Similarly, lineament density is inversely related to drainage density. The presence of lineaments, usually revealed in the form of fractures, joints, and cracks, especially in basement rocks, provides clues to groundwater potentials. These fractures, joints, and cracks when found in high density, provide good pathways through which water can saturate the openings in the rocks, thereby creating aquifers (Ahmed-II & Mansor, 2018). Land use and land cover, on the other hand, play an important role in controlling runoff, infiltration, and groundwater recharge (Krishnamurthy et al., 2000; Ogbonnaya et al., 2020). Land use types such as forested and vegetated lands encourage surface water infiltration and therefore increase the chances of groundwater recharge, while built-up areas, for example, encourage high runoff, therefore, retarding groundwater recharge (Shaban et al., 2006).

On the other hand, LULC provides vital information on how the influences of varying degrees of activities affect the capabilities of water infiltration (Krishnamurthy et al., 2000; Ogbonnaya et al., 2020).

Thematic layers of drainage density, lineament density, and slope were prepared from a mosaicked DEM and classified into four (4) regions, each based on the natural break classification scheme in the ArcGIS 10.5 computing environment. The LULC was prepared from mosaicked cloud-free Landsat OLI/TIRS images following the maximum likelihood supervised classification of the false-color composite of bands 5, 4, and 3 in the ENVI 5.3 computing environment.

Rainfall (RF) and Groundwater Level Fluctuation (GLF)

Rainfall is almost entirely the source of recharge to surface and groundwater in the Sokoto basin (Akudo et al., 2016). The measure of recharge to groundwater depends on the rainfall amount, intensity, and regularity. Areas with high and regular rainfall experience better recharge compared to those with low rainfall amounts and regularity (Ogbonnaya et al., 2020). This thematic layer was prepared by adopting the Thiessen polygon method in the ArcGIS 10.5 computing environment to create a spatial distribution map of rainfall. It was further categorized into four (4) zones according to the natural break classification to indicate high to low rainfall zones.

Groundwater level fluctuation (GLF) data spanning a long period provides reliable information on groundwater potential in an area. Because of this understanding, this work, contrary to that previously done in the basin (Kudamnya & Andongma, 2017), considered GLF a significant factor for identifying groundwater potential regions. GLF layer was prepared using the inverse distance weighted (IDW) technique in the ArcGIS 10.5 computing environment and further classified into 4 classes according to natural break classification.

Multi Influencing Factor (MIF) Method

Assigning weightage to factors influencing groundwater potential usually tends to be a subjective process whereby undue advantages are given to some factors, mostly based on speculation. The MIF method is one way of drastically reducing the subjectiveness of the weight-assigning procedure (Fig. 4). The advantage of this method over many others is its robustness in taking into consideration that all factors affecting a particular resource (e.g. groundwater), are interrelated and interdependent (Shaban et al., 2006; Nganga

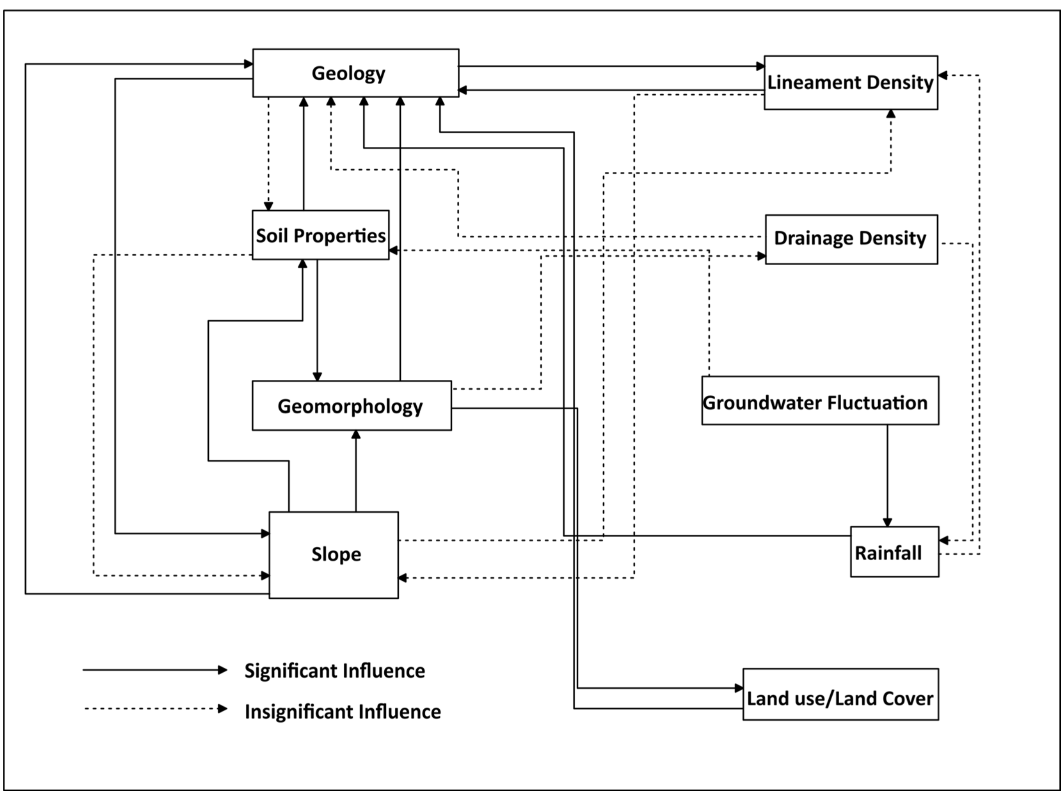

Fig. 4 Flow chart showing the associations between the multi-influential factors (MIF), selected for identifying the groundwater potential regions in the study area

Table 2 Significant, insignificant and cumulative sum of individual influencing factors

Factor	Significant influence (X)	Insignificant influence (Y)	Proposed relative rates $(X+Y)$	Proposed score of each influencing factor $[\frac{(X+Y)}{\sum(X+Y)}] * 100$	Approximated score
Geology	2	0.5	2.5	14.3	14
Lineament	1	0.5	1.5	8.6	9
Soil	2	0.5	2.5	14.3	14
Drainage	0	1	1.0	5.7	6
Geomorphology	2	0.5	2.5	14.3	14
Slope	3	0.5	3.5	20	20
GW fluctuation	1	0.5	1.5	8.6	9
Rainfall	1	0.5	1.5	8.6	9
Land use/land cover	1	0	1.0	5.7	6

et al., 2020; Magesh et al., 2012; Kaliraj et al., 2015; Thapa et al., 2017). The interrelationship between factors can have two effects: major and minor (Table 2). A major effect represents the direct influence of one factor over another and is assigned a value of 1.0, while the minor effect represents only the indirect influence of one factor over another and is assigned a value of 0.5. Slope factor, for instance, has a major relationship with geology, geomorphology, and soil with a minor influence on lineament. Thus, its evaluated weight is 3.5. The weight of a factor, therefore, depends on the cumulative scores of all its direct and indirect influences over other factors (Table 3) and can be represented using Eq. 1 (Raju et al., 2019).

$$MIF = \frac{x+y}{\sum(x+y)} \times 100 \quad (1)$$

where x represents the major effect between two factors and y represents the minor effect between two factors. Further details can be found in Shaban et al. (2006) and AKinwumiju et al. (2016).

Results and Discussion

From the thematic layers obtained (factor maps), each factor was categorized into 4 classes and expressed either numerically (as in the case of rainfall, lineament, drainage, slope, and groundwater fluctuation) or descriptively.

Geology (GE)

Groundwater occurrence, distribution, and movement depend largely on some characteristics of the rock, namely, porosity and permeability, which depend on the rock types (Etikala et al., 2019; Ghasemizadeh et al., 2012; Kogbe 1989). The area consists of the Gundumi formation, which is at the base of the sequence and on the southeastern part, with the Northeastern part largely comprising the Gwandu formation, while the Taloka and Wurno formations occupy the southern part (Fig. 5).

Adelana et al. (2006) classified the basin into eight geologic Formations:

(a) Gwandu Formation (sands and clay)
(b) Gamba Formation (shale and clay)
(c) Kalambaina Formation (limestones with joints and cavities)
(d) Dange Formation (shale and clay)
(e) Wurno Formation (sand, shale, and siltstone)
(f) Dukamaje Formation (shale and clay)
(g) Taloka Formation (sand, clay, and siltstone)
(h) Gundumi/Illo Formation (coarse sands and gravels)

The Formations occur below the Quaternary continental alluvium, consisting of sandy drifts and laterites, and are underlain by the Gundumi/Illo formation overlying the Precambrian basement complex in the Northeastern and Southeastern parts.

Geology is the 14th influencing factor used for the GWPR of the Sokoto Basin. Based on their groundwater prospects, the weights corresponding to the Formations are arranged as Gwandu (medium sandstone), Taloka and Wurno (medium to fine sandstone), Gundunmi (coarse sandstone), Alluvium, Kalambaina (limestone), Illo, Dange (shale and clay) and Dukamaje (shale and clay) (Table 3), respectively. The Gwandu Formation, consisting of medium sandstone, received a weight of 14, while Dukamaje, made up of shale and clays, received the lowest weight of 1.

Soil Properties (SP)

According to Das (2017), soil is a very influential factor concerning the rate and amount of water infiltration, especially

Table 3 Corresponding weights and ranks of individual factors influencing groundwater potential regions in the study area

Factor	Sub-class	Weightage	Rating
Geology	Gwandu (GWSS, GLCL, WSS)	14	14
	Taloka &Wurno	12	
	Gundunmi	10	
	Alluvium	8	
	Kalambaina	6	
	Illo formation	4	
	Dange	2	
	Dukamaje	1	
Lineament	0–2.64	1	9
	2.65–5.28	3	
	5.29–7.91	5	
	7.92–10.6	7	
	10.7–13.2	9	
Soil	Lithosols	8	14
	Hydromorphic	10	
	Ferruginous on sandy material	14	
	Ferruginous on undifferentiated material	4	
	Undifferentiated ferruginous	6	
Drainage	0–40.4	6	6
	40.5–80.9	5	
	81–121	4	
	122–162	3	
	163–202	2	
Geomorphology	Lowlands	14	14
	Pediplain	10	
	Hills and ridges	6	
Slope	0–4	20	20
	4.1–8	16	
	8.1–12	12	
	12.1–16	8	
	> 16	4	
GW fluctuation	4.5–17.45	9	9
	17.46–30.41	7	
	30.42–43.36	5	
	43.37–56.31	3	
	56.32–69.20	1	
Rainfall	100–150.48	1	9
	150.49–200.95	3	
	200.96–250.44	5	
	250.45–310.91	7	
	310.92–370.39	9	
Land use/land cover	Water bodies	6	6
	Vegetated areas	5	
	Cultivated areas	4	
	Bare-land	2	
	Built-up areas	1	

from precipitation to the subsurface to recharge aquifers. Porosity, permeability, texture, etc., can either inhibit or enhance the chances of water reaching the subsurface through pores to saturate aquifers.

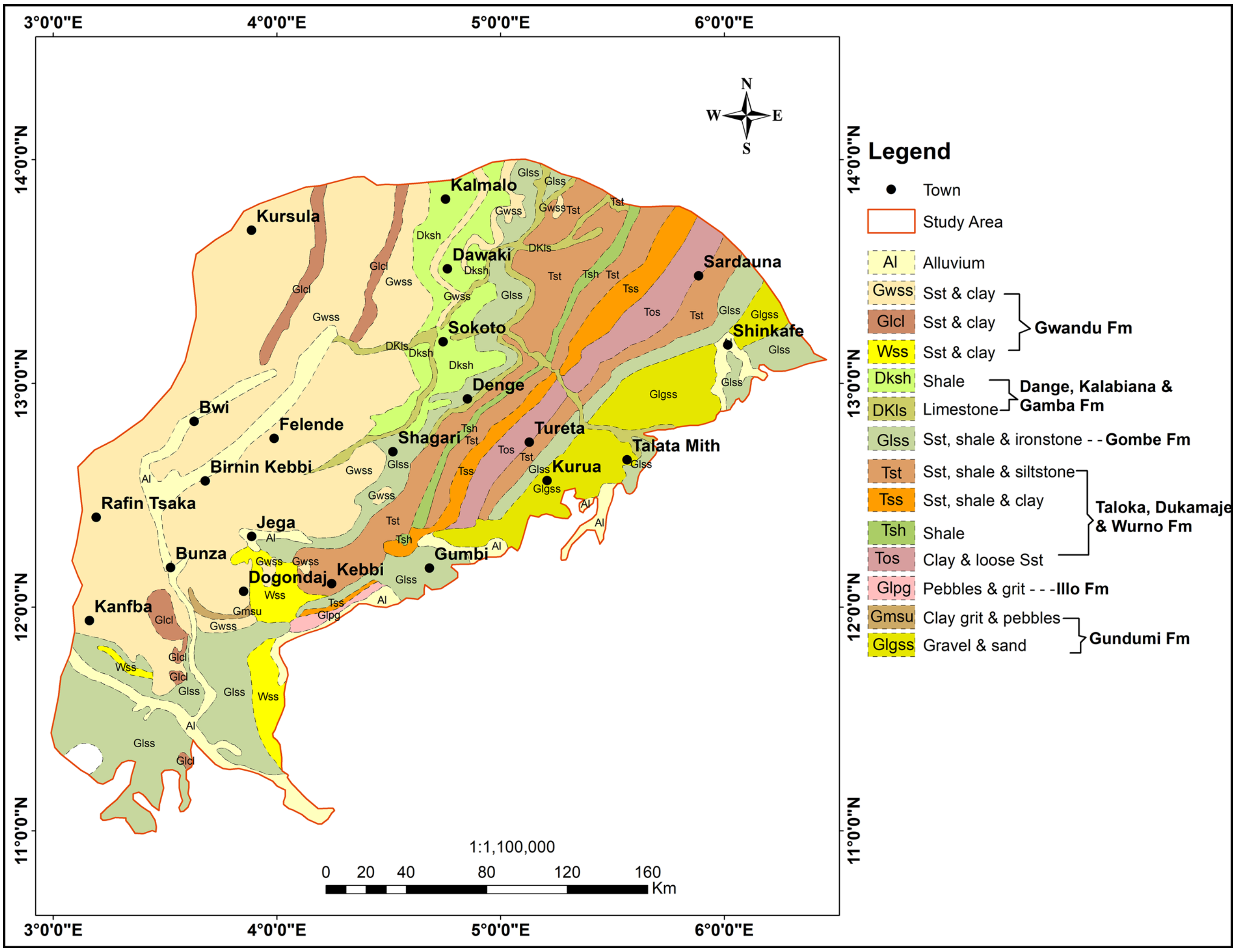

Fig. 5 Geologic map, depicting the formations and rock types in the study area

The soils are classified into five types (Fig. 6), which include lithosols, hydromorphic, ferruginous on sandy materials, ferruginous on undifferentiated materials, and undifferentiated ferruginous. Ferruginous on undifferentiated is the most abundant and occupies the central and Southeastern parts, constituting approximately 22,458.1 km^2 (35.7%). The ferruginous on sandy materials occurring north of the area cover about 14,521.21 km^2 (23.1%). Undifferentiated ferruginous, which occupies the southeastern and extends southwards, covers about 9,637.77 km^2 (15.3%). The remaining two soil types viz, lithosols found southwards, occupy about 9,865.2 km^2 (15.7%), and hydromorphic, occurring as a thin layer from north down south occupy about 6,406.38 km^2 (10.2%). Based on the water percolation and retention capabilities of the soils, suitable weights were given to the soils in descending order: ferruginous on sandy material (14), hydromorphic (10), lithosols (8), undifferentiated ferruginous (6), and ferruginous on undifferentiated (4) (Table 3), respectively.

Geomorphology (GM)

Geomorphology is defined by the geology of an area, and it provides clues for groundwater occurrence depending largely on the landforms observed (Waiker & Nilawar, 2014). The basin consists of a highly elevated area in the northern and northeastern parts, while the southern and central parts are nearly plain with gentle landforms. Based on the landforms, three geomorphologic features have been identified (Fig. 7). They include lowlands covering about 17,457.3 km^2 (27.8%), pediplains occupying an area of 28,632.8 km^2 (45.5%), and hills and ridges covering 16,798.6 km^2 (26.7%) of the area, respectively. Terrains that are weathered and fractured with a high elevation and steep landforms exhibit medium to low groundwater potentials (Raju et al., 2019); hence, the hills and ridges were assigned low weight. Lowlands and pediplains received high weightage accordingly. The lowlands, pediplains, hills, and ridges received 14, 10, and 6 (Table 3) as weights, respectively.

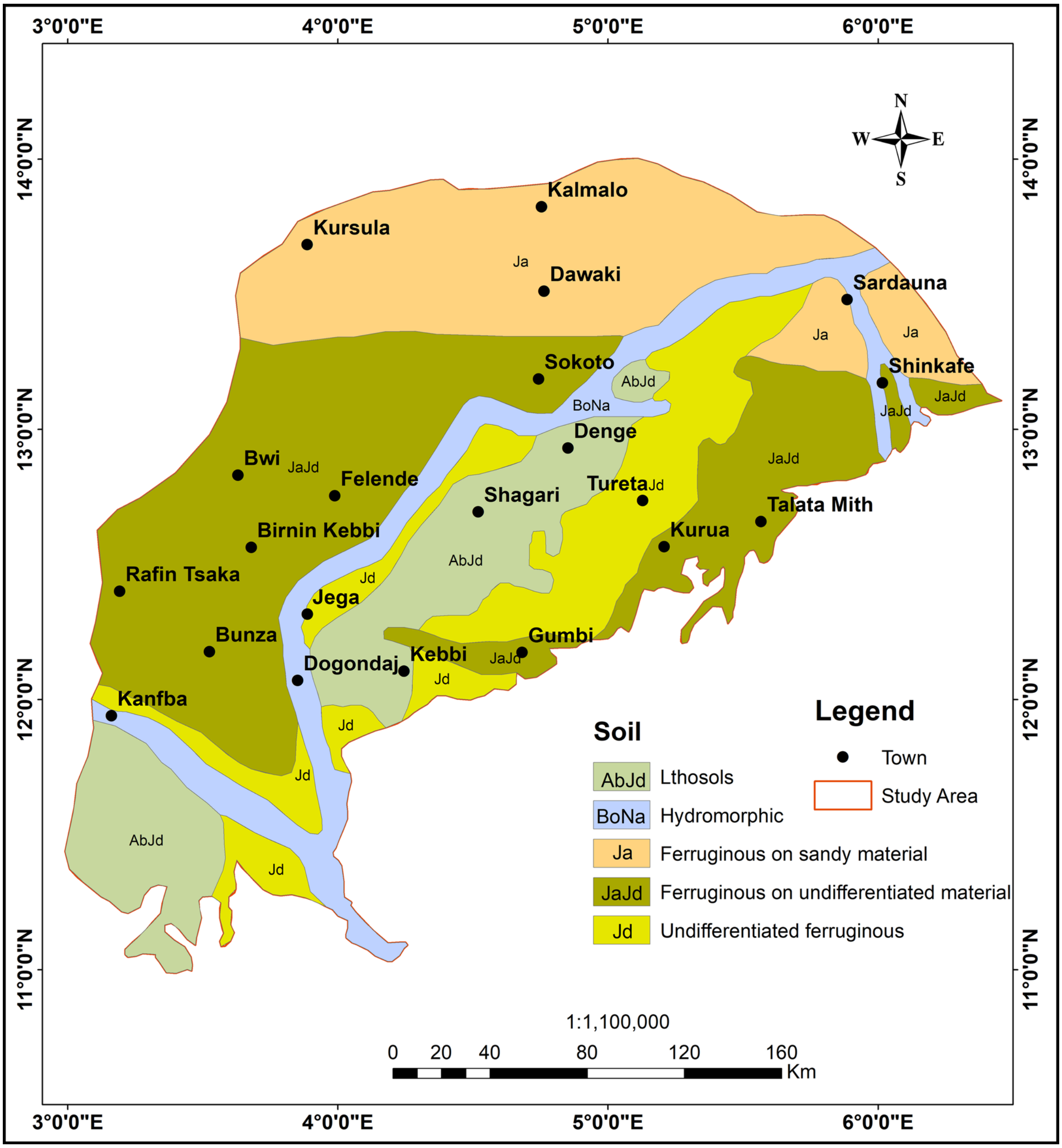

Fig. 6 Soil map, showing the classification of the soil types in the study area

Slope (SL)

The slope is among the major features that influence surface water retention time, infiltration, and recharge of aquifers. In places with a high slope, the rate and quantity of water that reaches the subsurface are highly reduced as surface runoff increases and surface water is not allowed to remain and gradually infiltrate into the subsurface. However, a low slope discourages surface runoff and increases retention time for surface water, thereby improving the prospect of water reaching the saturation zone to recharge the aquifer (Gabet & Sternberg, 2008). The slope classes in degrees are as follows (Fig. 8): 0–4 (nearly level), 4.1–8 (gently sloping), 8.1–12 (moderately sloping), 12.1–16 (moderately steep), and ˃16 (steeply sloping). The majority of the area consists of nearly level and gently sloping slopes, which elicit hope of groundwater occurrence. Based on that, the highest weightage was given to slopes of 0°–4° and 4.1°–8°, respectively. The lowest weights (Table 3) were subsequently given to slope ˃16°.

Lineament Density (LD)

Lineament density serves as a precursor for groundwater occurrences in an area. The presence of lineaments, which

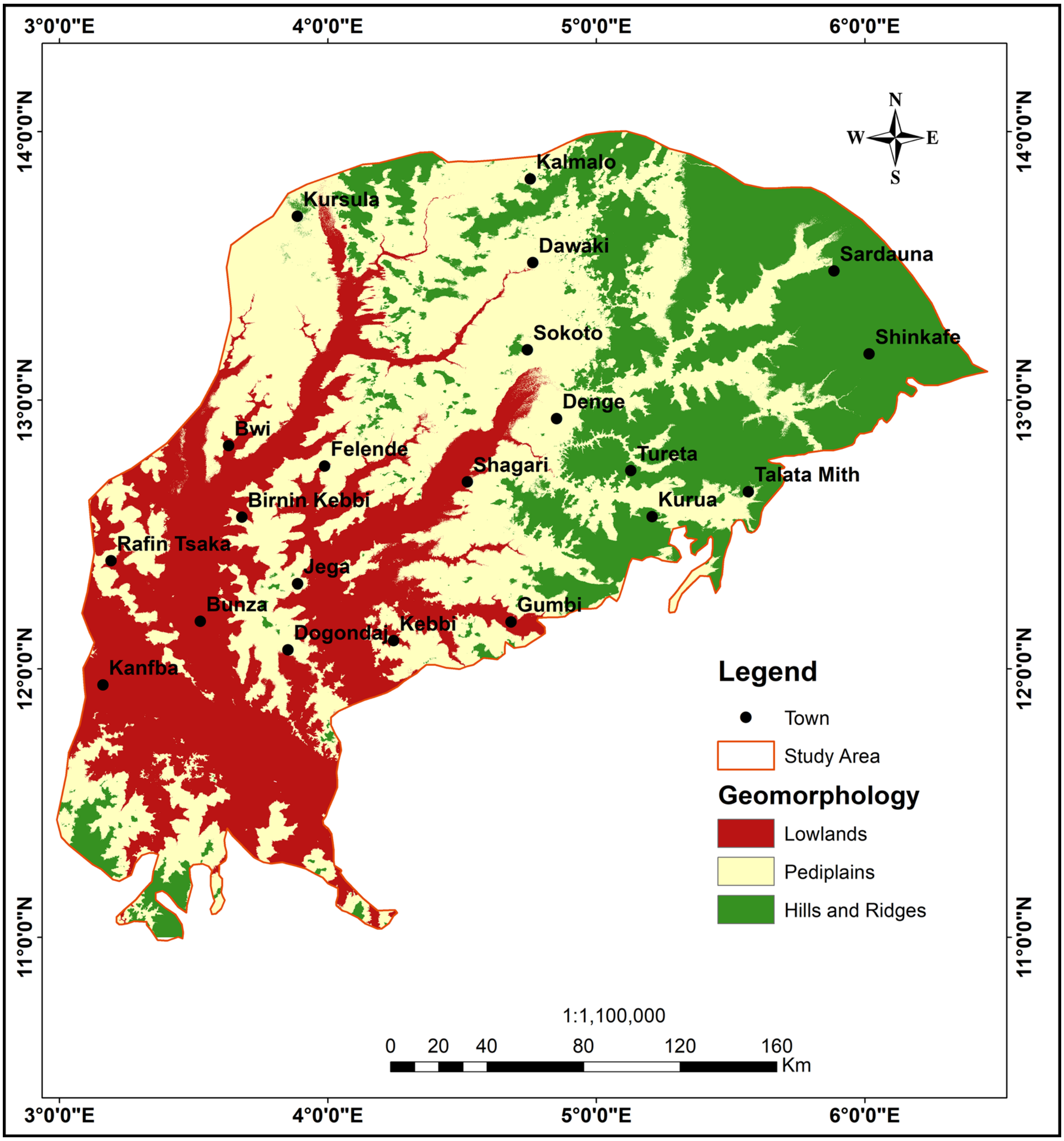

Fig. 7 Geomorphologic map, indicating the various types of landforms that characterize the study area

are usually revealed in the form of fractures, joints, and cracks, especially in basement rocks provides clues to groundwater potential. These fractures, joints, and cracks when found in high density, provide good pathways through which water can saturate the openings in the rocks, thereby creating aquifers (Ahmed-II & Mansor, 2018).

Figure 9 shows five lineament density classes: 0–2.64 km/km (low), 2.65–5.28 km/km (moderate), 5.29–7.91 km/km (moderately high), 7.92–10.6 km/km (high) and 10.7–13.2 km/km (very high). The area consists mainly of low lineament density, covering about 32,183.3 km^2 (51.2%). However, high lineament density accounts for only about 3,899.1 km^2 (6.2%), which is an indication of the absence of prolonged weathering in the area. Moderate lineament density occupies 12,766.4 km^2 (20.3%), moderately high accounts for about 7,861.1 km^2 (12.5%), and very high occupies about 6,178.1 km^2 (9.8%), respectively. The very high lineament density class was assigned a high rank, while the low lineament density class was ranked low (Table 3).

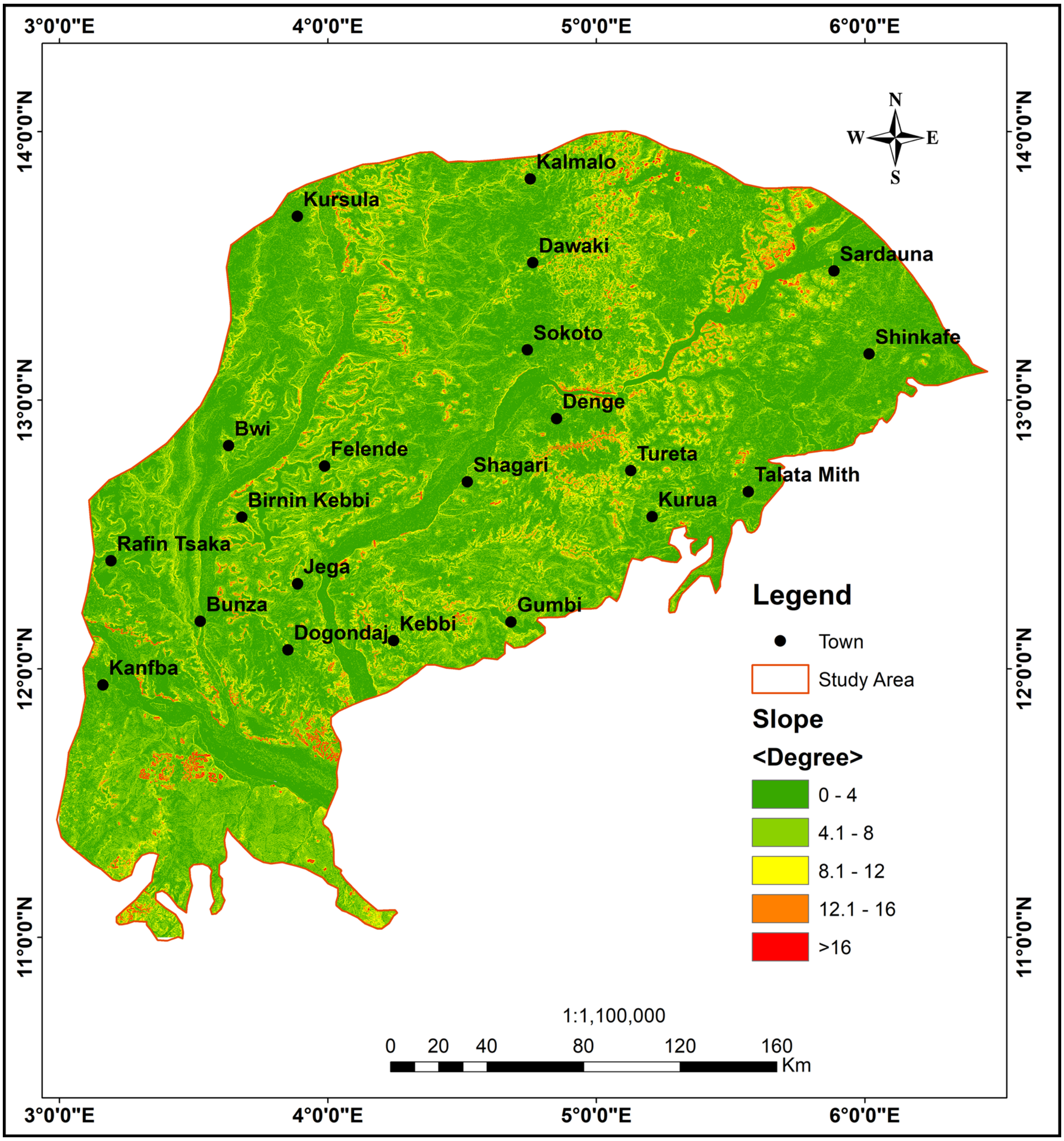

Fig. 8 Slope map, which categorized the slope classes in the study area

Drainage Density (DD)

Drainage is an expression of surface water channels and interconnectivity. Drainage density is related to slope and surface runoff, in the sense that an area with high drainage density usually has a high slope (steep-slope) and high surface runoff. Such areas with high slope density always have low water infiltration rates because the fast movement of water decreases the retention time required for better infiltration to occur. Low drainage density is rather synonymous with areas of gentle slope and low surface runoff, allowing enough retention time for water to infiltrate the subsurface. It is reasonable to associate low drainage density in lowlands with permeable and porous lithology and high groundwater potential. Unweathered lithology with low permeability and porosity, related mostly to basement complex areas, often has poor prospects for groundwater occurrence.

The area is grouped into five classes, namely: 0–40.4 km/km^2 (low), 40.5–80.9 km/km^2 (moderate), 81–121 km/km^2 (moderately high), 122–162 km/km^2 (high), and 162–202 km/km^2 (very high) (Fig. 10). Areas with low drainage density are aligned to certain geomorphic features such as lowlands, low runoff, high permeability, and porosity and encourage high infiltration and recharge potentials of the water. As such, areas with a low drainage density, covering

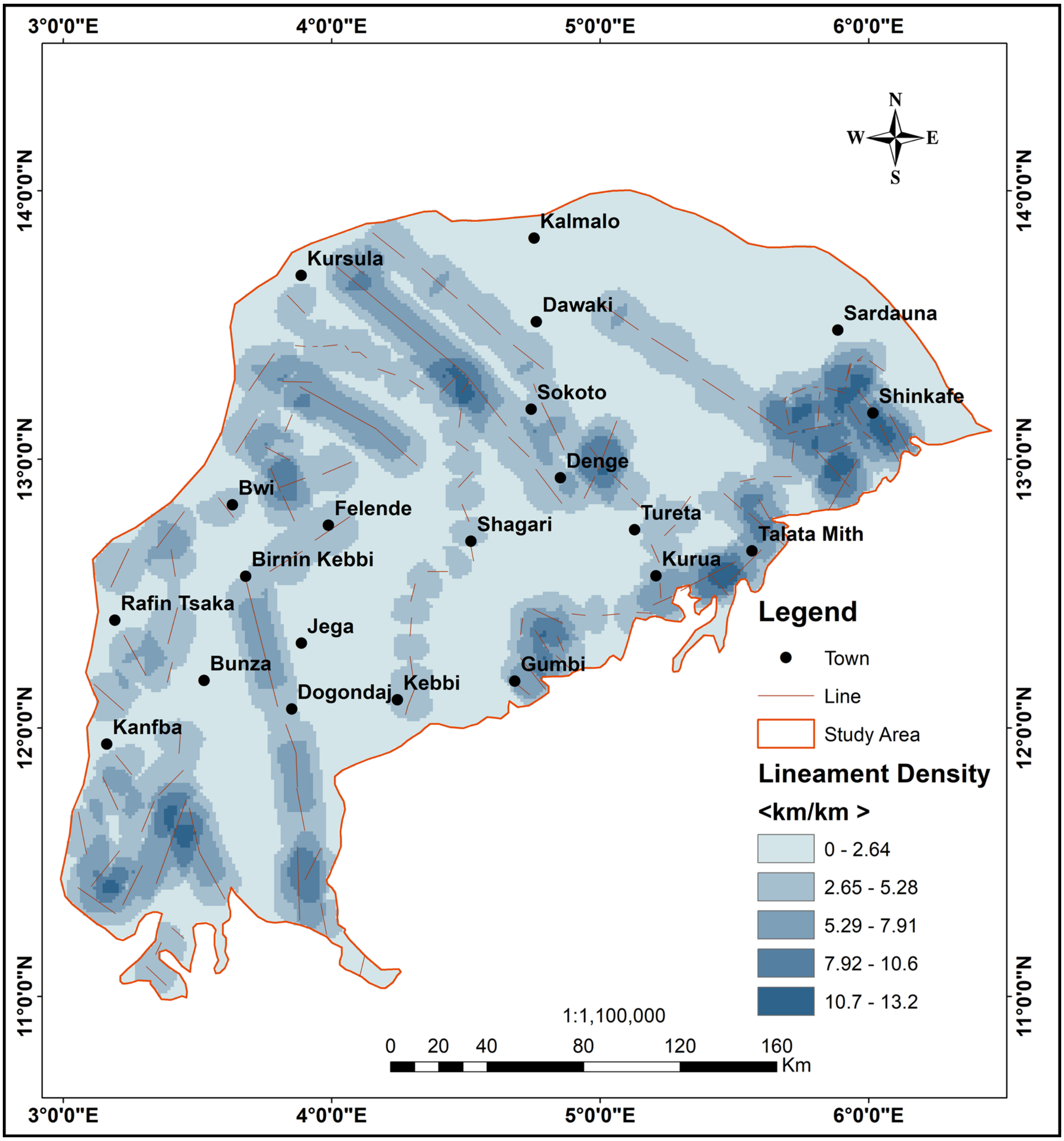

Fig. 9 Lineament density map, indicating the lineament classes in the study area

about 25,346.1 km^2 (40.3%), received a high weightage. Areas with a very high drainage density, accounting for about 5,445.3 km^2 (8.7%), were assigned the lowest weightage when compared to all other areas. Areas with moderate drainage density occupy about 17,823.8 km^2 (28.3%), moderately high covers about 10,064.3 km^2 (16.0%), and high drainage density covering about 4,209.5 km^2 (6.7%), respectively, were assigned weights accordingly.

Rainfall (RF)

In the Sokoto Basin, rainfall is almost entirely the source of recharge for surface and groundwater (Akudo et al., 2016). The measure of recharge to groundwater depends on the rainfall amount, intensity, and regularity. Areas with high and regular rainfall experience better recharge compared to those with low rainfall amounts and regularity (Ogbonnaya et al., 2020). The average annual rainfall in the basin ranges from 100 mm-370 mm, suggesting a semi-arid basin. Yearly average rainfall data comprising a 10 year period were obtained within ten sites of the NIMET locations stationed within the basin and processed using the Thiessen polygon method in the ArcGIS 10.5 software environment to generate rainfall distribution patterns (Fig. 11).This procedure categorized annual average rainfall into very high (310.92–370.39 mm), high (260.45–310.91 mm), moderate

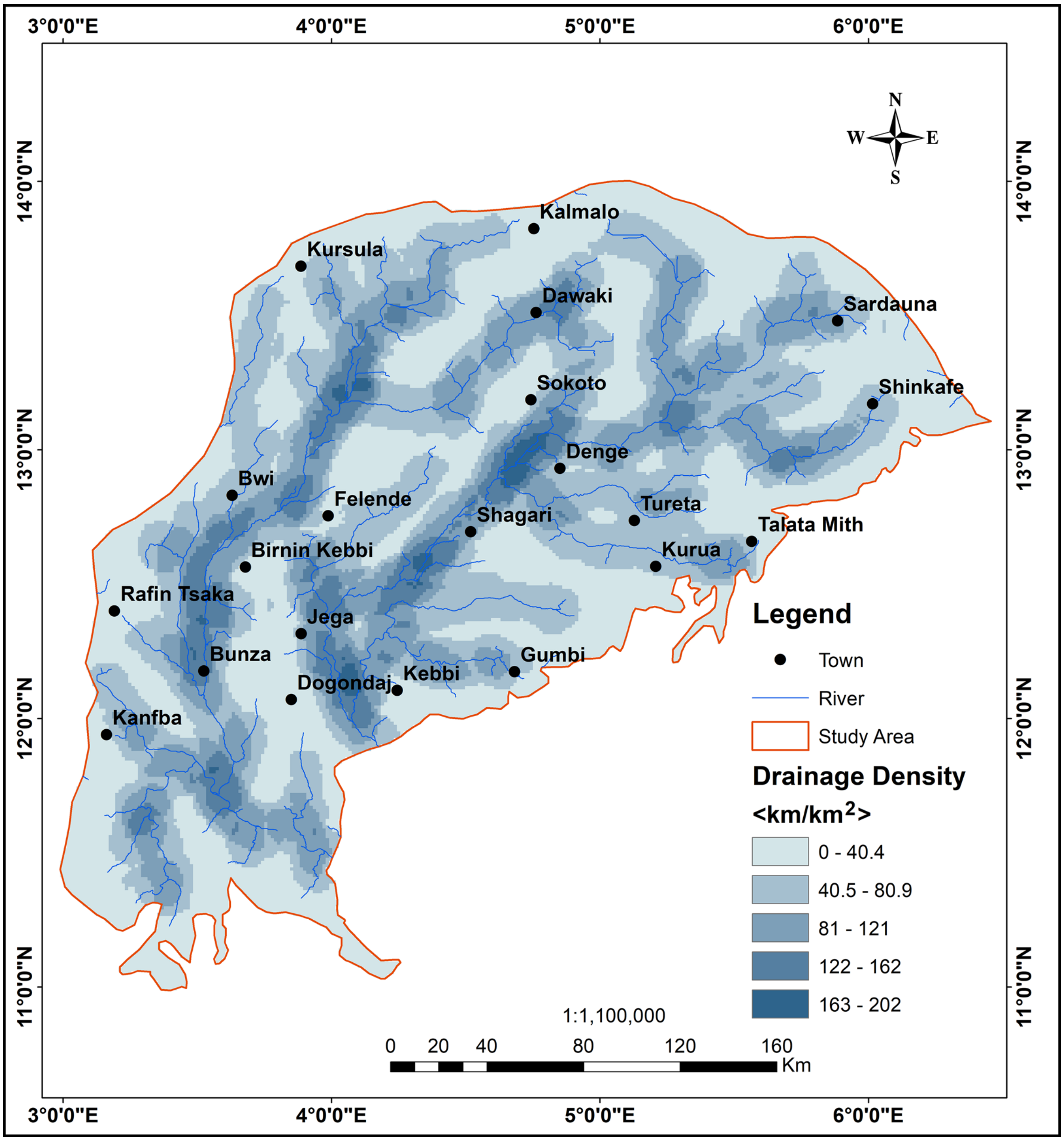

Fig. 10 Drainage density map, showing the drainage density classes, defined by the surface water interconnectivity in the study area

(200.97–260.96 mm), low (150.49–200.96 mm), and very low (100–150.48 mm), covering about 171.2 km^2 (0.28%), 22.7 km^2 (0.05%), 284.2 km^2 (0.46%), 7443.7 km^2 (11.8%), and 54,966.9 km^2 (87.4%), respectively. The regions with high rainfall were allocated high weightage, while regions with low rainfall were allocated lower weight ratings.

Land Use/Land Cover (LULC)

According to Krishnamurthy et al. (2000) and Ogbonnaya et al. (2020), the land use/land cover map provides vital information on how the influences of varying degrees of LULC activities affect the capabilities for water infiltration. The LULC map was generated through the unsupervised categorization of the false-color composite of the bands 4, 3, and 2 to obtain the LULC classes. The area consists of five different LULC classes, namely, built-up, vegetated, bareland, cultivated, and water bodies, respectively (Fig. 12). Water bodies were assigned the highest weight of 6 then followed by vegetated areas, which received 5, while cultivated areas got 4 as weight because the roots of crops, trees, and weeds alter soil bonds and create pathways for increased water infiltration (Ahmed, 2016). Bareland and built-up areas were ascribed low weights of 2 and 1, respectively, because the topsoil is often removed due to development purposes, thereby

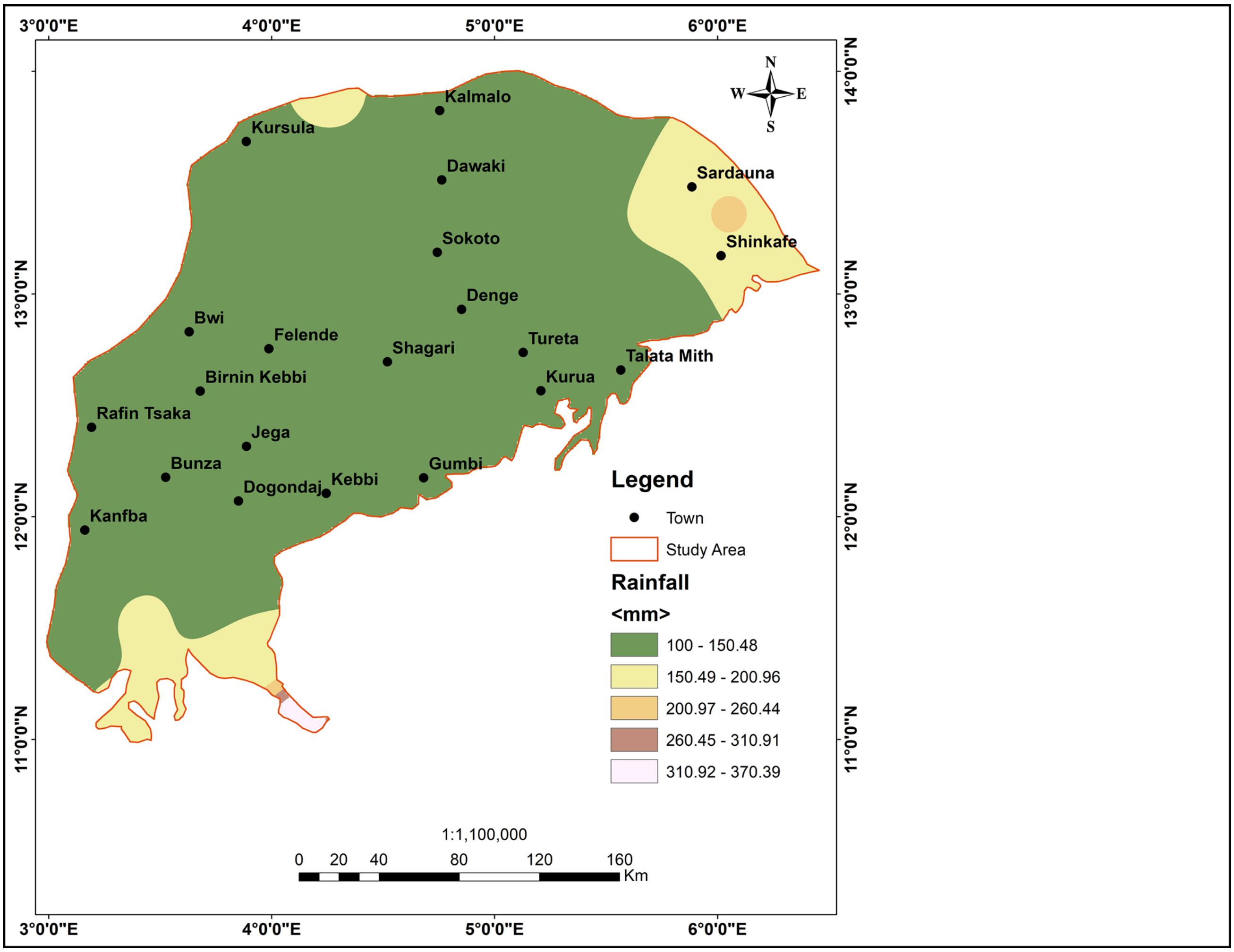

Fig. 11 Rainfall map, showing the rainfall distribution patterns for ten years (2002–2011) in the study area. (source: NIMET)

reducing water infiltration (Prabhu & Venkateswaran, 2015) (Table 3).

Groundwater Level (GL)

Groundwater level fluctuation data monitoring spanning a long period supplies reliable information on groundwater potentials in an area. Because of this understanding, this work, contrary to that previously done in the basin (Kudamnya & Andongma, 2017), considered GLF a significant factor for identifying groundwater potential regions. Groundwater level fluctuation (GLF) data were gathered in two ways. Basically, 5 years of GLF data were obtained from the Sokoto State Water Cooperation. From Fig. 13, the average depth to water level ranges between 4.50 and 69.26 m. The GLF were categorized into 5 classes which include: very high (56.32–69.26 m), high (43.37–56.31 m), moderate (30.42–43.36 m), low (17.46 – 30.41 m), and very low (4.503–17.45 m), with area coverage of approximately 241.3 km^2 (0.38%), 11,916.2 km^2 (18.9%), 27,986.4 km^2 (44.5%), 15,975.2 km^2 (25.4%), and 6,769.6 km^2 (10.8%), respectively. Regions with high groundwater level fluctuations were allocated low weight, while regions with low groundwater level fluctuations received high weightage (Table 3).

Groundwater Potential Regions (GWPR)

The final GWPR map was generated using an assemblage of the entire nine (9) factors (geology, soil properties, geomorphology, slope, lineament density, drainage density, rainfall, land use land cover, and groundwater level fluctuation) and their classes utilizing the Weighted Linear Combination technique in the raster calculator of the ArcGIS 10.5 software environment using Eq. (2).

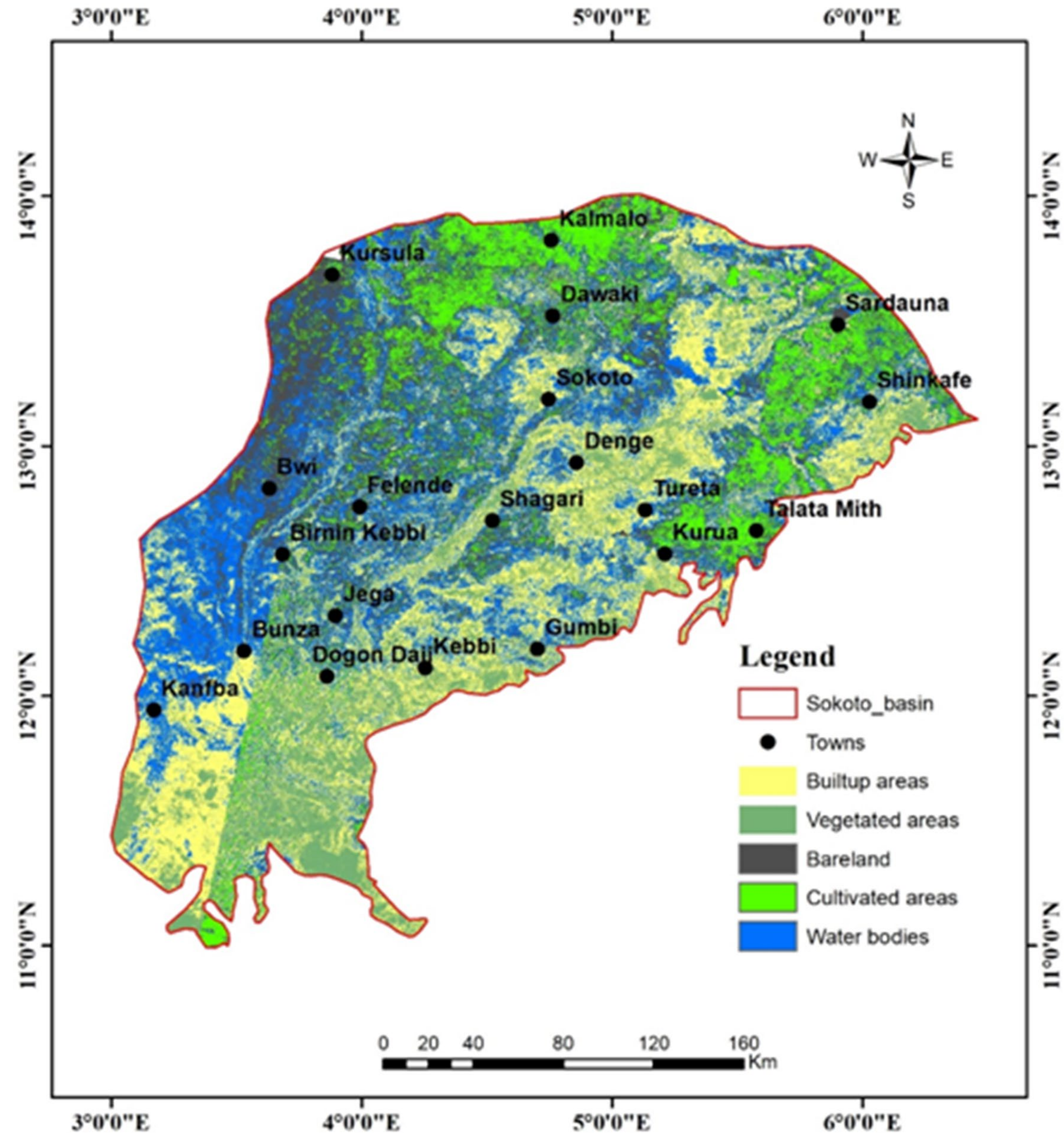

Fig. 12 Land use/land cover map, indicating the different LULC classes in the study area

$$\text{GWPR} = \sum_{i}^{n} (\text{GEw} * \text{GEr}) + (\text{SPw} * \text{SPr}) + (\text{GMw} * \text{GMr}) + (\text{SLw} * \text{SLr}) + (\text{LDw} * \text{LDr}) + (\text{DDw} * \text{DDr}) + (\text{RFw} * \text{REr}) + (\text{LULCw} + \text{LCLUr}) + (\text{GLFw} + \text{GLFr}) \tag{2}$$

where GWPR is the groundwater potential regions, GE is geology, SP is soil properties, GM is geomorphology, SL is the slope, LD is lineament density, DD is drainage density, RF is rainfall, LULC is land use/land cover, and GLF is groundwater level fluctuation, w is individual weights, and r is the rating of each influential factor.

After applying the weighted overlay and multi-influencing factor techniques, the Sokoto basin was divided into four GWPRs. These classes include poor, moderate, good, and very good groundwater potential regions, with spatial expanse of 17.4 km^2 (0.028%), 34,470.6 km^2 (54.8%), 26,380.2 km^2 (42.0%), and 2,020.5 km^2 (3.2%) in the order given (Fig. 14). From the GWPR map, more than half of the basin (54.8%) has moderate and poor potentials within the Northern part of the basin, while the southern part of the basin has good and very good potentials.

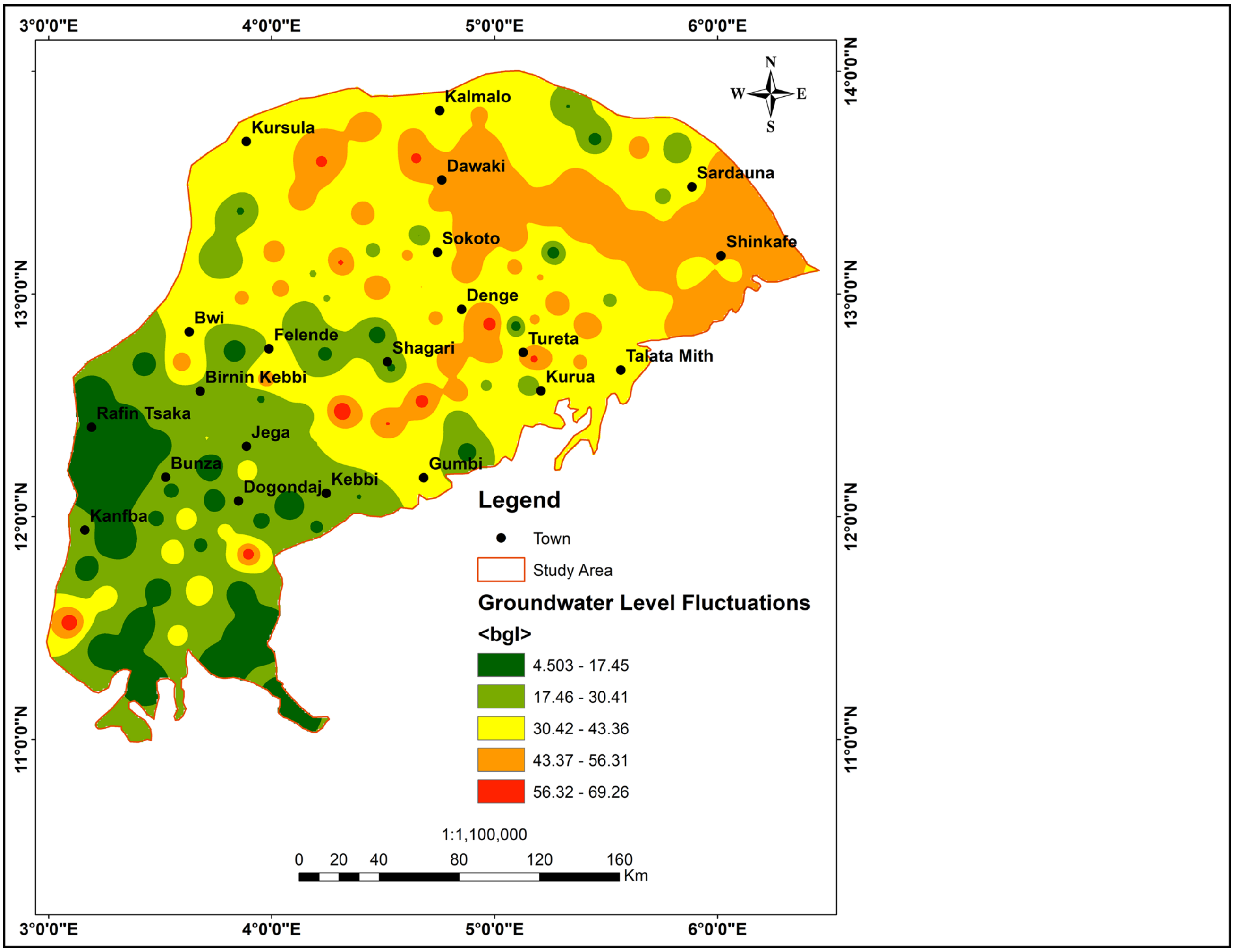

Fig. 13 Groundwater level fluctuation map, revealing the changes in the average depth to water level in monitoring wells in the study area. ((source: Sokoto State Water Corporation)

Results Validation

For a modeling task to be adjudged successful or otherwise, the results must be compared to a physically measurable parameter or subjected to some form of mathematical/statistical relationship (Ostad-Ali-Askari et al., 2017; Zealand et al., 1999). One of the most reliable approaches to authenticate/validate models of groundwater potential is to compare the results with available well yields estimated through pumping tests in the study area. To validate the exactness of the GWPR map produced with the GIS and MIF techniques, existing borehole data (well yield) from 45 boreholes were assembled in the study area (Table 1). The borehole depths range from 35–80 m, and the aquifer thickness ranges between 3.3 to 12 m. The existing well yields fall within a range of 0.5 l/s–6.0 l/s, and relying on the yield values, they were arranged into four (4) classes. These classes range from 0–2 l/s, 2.1–4.0 l/s, 4.1–6.0 l/s, and ˃6 l/s, referred to as poor, moderate, good, and very good yield, respectively. This classification matches the grouping of the groundwater potential regions achieved using GIS and MIS techniques, revealing the agreement between the GWPR map and existing borehole yield from a pumping test. Borehole data were superimposed on the groundwater potential map, and the number of wells corresponding to different groundwater potential regions was analyzed. Boreholes with very good to good yield were found in the sandstone, while boreholes of moderate yield were found within the limestone areas. Low yields are found in areas made of shale and clay materials.

A further accuracy evaluation was undertaken to certify the correlation between existing well data and the generated map of the groundwater potential regions. Following published procedures (Jensen, 1996; Raju et al., 2019), the error matrix or Confucius matrix (Eq. 3) is useful for verifying the correctness of the research outcomes by taking existing well

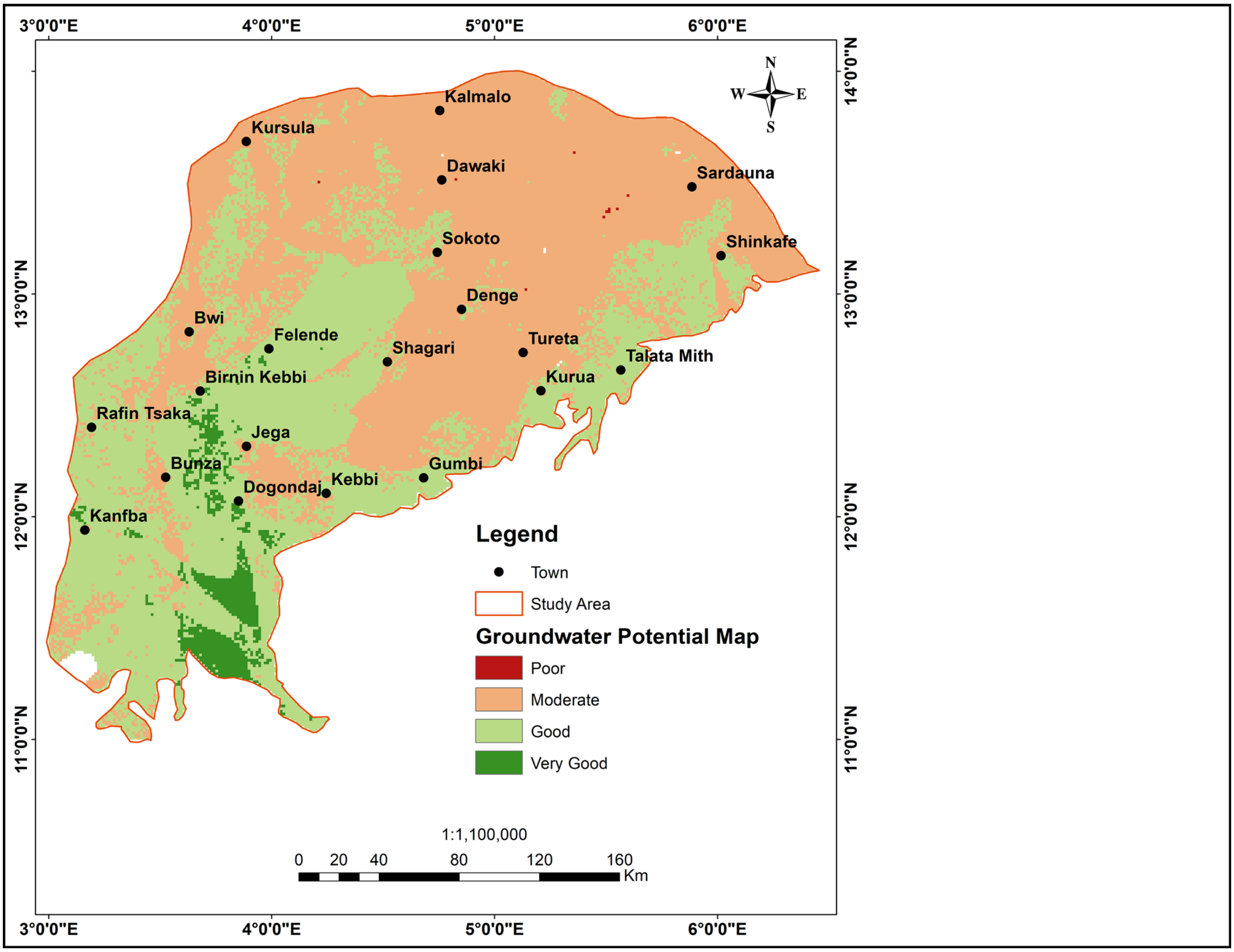

Fig. 14 Groundwater potential regions map, showing four groundwater potential classes in the study area, generated by utilizing WOM and MIF techniques

Table 4 Computed error matrix for validation of GWPR map

S/N	GWPR	Poor	Moderate	Good	Very good	Total	Total correct
1	Poor	2	3	0	0	5	2
2	Moderate	3	12	0	2	17	12
3	Good	0	3	12	1	16	12
5	Very good	0	0	1	6	7	6
	Total	5	18	13	9	45	32

Overall accuracy = 32/45*100% = 71.1%

data as reference points. Table 4 shows the overall accuracy of the data input and the results computed from the formula below;

$$Overall\ accuracy = \frac{No.\ of\ correct\ EWL}{Total\ No.\ of.\ EWL} = \frac{32}{45} * 100\% = 71.1\% \tag{3}$$

where EWL is existing well locations.

The overall computed accuracy using an error matrix of 71.1% substantially agrees with the results obtained from GIS and MIF techniques.

Conclusion

The present study investigated groundwater potentials for the Sokoto basin using an integrated approach of GIS and MIF techniques. The MIF was chosen to decide the factors that have significant influence and those that have insignificant influence on groundwater occurrence and movement in the study area. Nine GWPR factors of geology, soil property, geomorphology, slope, lineament density, drainage density, rainfall, land use/land cover, and groundwater level fluctuation were chosen, evaluated, and prepared into thematic maps using different methods. These thematic layers were then overlaid on the GIS environment, and the Multi-Influence Factor (MIF) analysis techniques and the weighted overlay method were then used to assign weights, and the groundwater potential map of the study area was generated. The GWPR map of the study area was categorized into very good potentials, good potentials, moderate potentials, and poor groundwater potentials. The very good, good, moderate, and poor potentials occupy spatial extent of 17.4 km^2 (0.028%), 34,470.6 km^2 (54.8%), 26,380.2 km^2 (42.0%), and 2,020.5 km^2 (3.2%), respectively. This indicates that the area largely possesses good and moderate groundwater potential. Next, the accuracy and reliability of the GWPR map were validated in comparison to existing borehole yield data covering most of the study area. The range of the yields are 0–2 l/s, 2.1–4.0 l/s, 4.1–6.0 l/s, and ˃6 l/s representing poor, moderate, good, and very good yields, respectively. The GWPR maps produced from the integration of GIS and MIF techniques concur substantially with the existing borehole yields, showing that modeling with the above techniques was very authentic and recommended for deployment in other areas for similar studies. Because groundwater resources in the study area are likely to continue to decline, as reflected by the lowering of the water table owing to low precipitation and increased usage of water for domestic and agricultural purposes, etc., groundwater monitoring and proper management of the resource is expedient.

Acknowledgements The authors appreciate NIMET and Sokoto State Water Corporation for providing part of the data used to accomplish this research.

Author's Contributions Authors have contributed immensely to the completion of the manuscript. EO, S.I, JA, and GA all worked together during the research compilation and discussion of this article.

Data Availability All data generated or analyzed during this study are included in this article.

Declarations

Conflict of interest No relevant financial or non-financial interests exist for the authors to disclose.

References

Abdullahi, B. U., Rai, J. K., Momoh, M., & Udensi, E. E. (2013). Application of remote sensing and GIS in groundwater mapping in some selected localities in Kebbi State, Nigeria. *International Journal of Marine, Atmosphere & Earth Sciences, 1*(2), 81–95.

Abdullahi, S. A., Muhammad, M. M., Adeogun, B. K., & Mohammed, I. U. (2014). Assessment of water availability in the Sokoto Rima River Basin. *Resources and Environment, 4*(5), 220–233. https://doi.org/10.5923/j.re.20140405.03

Adamu, A. (2019). Electrical resistivity mapping of aquiferous zones within Gudi-takalau area of Birnin Kebbi, Nigeria. *ATBU Journal of Environmental Technology, 12*(1), 29–46.

Adelana, S. M. A., Olasehinde, P. I., & Vrbja, P. (2006). A quantitative estimation of groundwater recharge in part of the Sokoto Basin, Nigeria. *Journal of Environmental Hydrology, 14*(5), 1–16.

Adelana, S. M. A., Olasehinde, P. I., & Vrbka, P. (2003). Isotope and geochemical characterization of surface and subsurface waters in semi-arid Sokoto Basin, Nigeria. *African journal of Science and technology, Science and Engineering Series, 4*(2), 80–89. https://doi.org/10.4314/ajst.v4i2.15298

Ahmed, J. B., II., & Mansor, S. (2018). overview of the application of geospatial technology to groundwater potential mapping in Nigeria. *Arabian Journal of Geosciences, 11*(17), 504. https://doi.org/10.1007/s12517-018-3852-4

Ahmed, J. B., II., & Pradhan, B. (2019). Spatial assessment of termites interaction with groundwater potential conditioning parameters in Keffi, Nigeria. *Journal of Hydrology, 578*, 1–17. https://doi.org/10.1016/j.jhydrol.2019.124012

Ahmed, S. A. (2016). Geospatial technology for delineating groundwater potential zones in Doddahalla watershed of Chitradurga district, India. *The Egyptian Journal of Remote Sensing and Space Sciences, 19*(2), 223–234. https://doi.org/10.1016/j.ejrs.2016.06.002

Akinbiyi, O. A., Oladunjoye, M. A., Sanuade, O. A., & Oyedeji, O. (2019). Geophysical Characterization and hydraulic properties of unconsolidated floodplain aquifer system in Wamako area, Sokoto, north-western Nigeria. *Applied Water Science, 9*(8), 1–10. https://doi.org/10.1007/s13201-019-1065-y

Akinwumiju, A. S., Olorunfemi, M. O., & Afolabi, O. (2016). GIS-based integrated groundwater potential assessment of Osun drainage basin, Southwestern Nigeria. *Ife Journal of Science, 18*(1), 147–168.

Akudo, E. O., Egboka, B. C. E., & Okpara, S. O. (2016). Estimation of groundwater recharge in Sokoto basin, using the water table fluctuation method. *Journal of Scientific and Engineering Research, 3*(1), 25–33.

Akudo, E. O., Ozulu, G. U., & Osogbue, L. E. (2010). Quality assessments of groundwater from Selected refuse dumpsites areas in Warri. *Environmental Research Journal, 4*(4), 281–285. https://doi.org/10.3923/erj.2010.281.285

Akujieze, C. N., Coker, S. L. J., & Oteze, G. E. (2003). Groundwater in Nigeria—a millennium experience—Distribution, practice, problems and solutions. *Hydrogeology, 11*, 259–274. https://doi.org/10.1007/s1004-002-0227-3

Al-Abadi, A. M., Shahid, S., Ghalib, H. B., & Handhal, A. M. (2017). A GIS-based integrated fuzzy logic and analytic hierarchy process model for assessing water-harvesting zones in Northeastern Maysan Governorate, Iraq. *Arabian Journal for Science and Engineering, 42*(6), 2487–2499.

Allafta, H., Opp, C., & Patra, S. (2020). Identification of groundwater potential zones using remote sensing and GIS techniques: A case study of the Shatt Al-Arab Basin. *Remote Sensing, 13*(1), 112.

Das, S. (2017). Delineation of groundwater potential zone in hard rock terrain in Gangajalghati block, Bankura district, India using remote sensing and GIS techniques. *Modeling Earth Systems and Environment, 3*(4), 1589–1599.

Das, S., & Pardeshi, S. D. (2018). Integration of different influencing factors in GIS to delineate groundwater potential areas using IF and FR techniques: A study of Pravara basin, Maharashtra, India. *Applied Water Science, 8*, 197. https://doi.org/10.1007/s13201-018-0848-x

Ekpoh, I. J., & Ekpenyong, N. (2011). The effects of recent climatic variations on water yield in the Sokoto region of Northern Nigeria. *International Journal of Business and Social Science, 2*(7), 251–255.

Etikala, B., Golla, V., Li, P., & Renati, S. (2019). Deciphering groundwater potential zones using MIF technique. A study from Tirupati area, Chittoor District, Andhra Pradesh, India. *Hydro Research, 1*, 1–7. https://doi.org/10.1016/j.hydres.2019.04.001

Food and Agricultural Organization (FAO). (1995). Soil and water resources survey of Sokoto valley. *Nigeria. Climate and Hydrology, 4*, 85p.

Gabet, E. J., & Sternberg, P. (2008). The effects of vegetative ash on infiltration capacity, sediment transport, and the generation of progressively bulked debris flows. *Geomorphology, 101*(4), 666–673. https://doi.org/10.1016/J.GEOMORP.2008.03.005

Ghasemizadeh, R., Hellweger, F., Butscher, C., Padilla, I., Vesper, D., Field, M., & Alshawabkeh, A. (2012). Review: Groundwater flow and transport modeling of karst aquifers, with particular reference to the North Coast limestone aquifer system of Puerto Rico. *Hydrogeol Journal, 20*(8), 1441–1461. https://doi.org/10.1007/s10040-012-0897-4

Goni, I. B. (2006). The challenges of meeting domestic water supply in Nigeria. *Journal of Mining and Geology, 42*(1), 51–55.

Gupta, M., & Srivastava, P. K. (2010). Integrating GIS and remote sensing for identification of groundwater potential zones in the hilly terrain of Pavagarh, Gujarat, India. *Water International, 35*(2), 233–245.

Guru, B., Karthik, S., & Somnath, B. (2017). Frequency ratio model for groundwater potential mapping and its sustainable management in cold desert, India. *Journal of King Saud University - Science, 29*(3), 333–347.

Hamidu, H., Garba, M. L., Abubakar, Y. I., Muhammad, U., & Muhammed, D. (2016). Groundwater resources appraisals of Bodinga and Environs, Sokoto basin north western Nigeria. *Nigerian Journal of Basic and Applied Sciences, 24*(2), 92–101. https://doi.org/10.4314/njbas.v24i2.13

Hanidu, J. A. (1990). National growth, water demand and supply strategies in Nigeria in the 1990s. *Water Resources, 2*(1), 1–6.

Ifediegwu, S. I. (2022). Assessment of groundwater potential zones using GIS and AHP techniques: A case study of the Lafia district, Nasarawa State, Nigeria. *Applied Water Science, 12*(10), 1–17. https://doi.org/10.1007/s13201-021-01556-5

Ifediegwu, S. I., Nnebedum, D. O., & Nwatarah, A. N. (2019). Identification of groundwater potentials zones in the hard and soft rock terrains of Kogi State, North Central Nigeria: An integrated GIS and remote sensing techniques. *SN Applied Sciences, 6*, 1151. https://doi.org/10.1007/s42452-019-1181-1

Igor, S. (1993). World freshwater resources. In P. H. Gleick (Ed.), *Water in crisis: A guide to the world's freshwater resources* (pp. 13–24). Oxford University Press.

Jensen, J. R. (1996). *Introductory digital image processing: A remote sensing perspective* (2nd ed.). Prentice Hill Inc.

Kaliraj, S., Chandrasekar, N., & Magesh, N. S. (2015). Evaluation of multiple environmental factors for site-specific groundwater recharge structures in the Vaigai River upper basin, Tamil Nadu, India, using GIS-based weighted overlay analysis. *Environment and Earth Science, 74*(5), 4355–4380. https://doi.org/10.1007/s12665-015-4384-9

Kogbe, C. A. (1989). Cretaceous and tertiary Iullemenden Basin in Nigeria. In C. A. Kogbe (Ed.), *Geology of Nigeria* (pp. 377–421). Jos rock New Pub Co.

Krishnamurthy, J., Mani, A., Jayaraman, V., & Manive, M. (2000). Groundwater resources development in hard rock terrain an approach using remote sensing and GIS techniques. *International Journal of Applied Earth Observation and Geoinformation, 2*(3/4), 204–215.

Kudamnya, E. A., & Andongma, W. T. (2017). Predictive mapping for groundwater within Sokoto Basin, North Western Nigeria. *Journal of Geography, Environment and Earth Science international, 10*(2), 1–14. https://doi.org/10.9734/JGEESI/2017/32440

Lakshmi, D. S. V., & Reddy, Y. V. K. (2018). Identification of groundwater potential zones using GIS and remote sensing. *International Journal of Pure and Applied Mathematics, 119*(17), 3195–3210.

Maduabuchi, C. M. (2004). Case studies on Transboundary aquifers in Nigeria. In: Bo Apelgren (Eds), *Managing shared aquifer resources in Africa*. IHP-IV, series on groundwater No. 8 (pp. 122-128).

Magesh, N. S., Chandrasekar, N., & Soundranayagam, J. P. (2012). Delineation of groundwater potential zones in Theni district, Tamil Nadu, using remote sensing. GIS and MIF Techniques. *Geoscience Frontiers, 3*(2), 189–196. https://doi.org/10.1016/j.gsf.2011.10.007

Manap, M. A., Sulaiman, W. N. A., Ramli, M. F., Pradhan, B., & Surip, N. (2013). A knowledge-driven GIS modeling technique for groundwater potential mapping at the Upper Langat Basin, Malaysia. *Arabian Journal of Geosciences, 6*(5), 1621–1637. https://doi.org/10.1007/s12517-011-0469-2

Miller, J. R., Ritter, D. F., & Craig, K. R. (1990). Morphometric assessment of lithologic controls on drainage basin evolution in the Crawford upland, south-central Indiana. *American Journal of Science, 290*, 569–599.

Musa, I. K. (1997). *Sustainable Irrigation Development and Management of water resources*. Paper presented at a symposium to mark the first National Irrigation Week, Kano.

Musa, A., & Mohammed, I. U. (2015). Geophysical investigations of lithology and groundwater potentials of recharge zones. *International Journal of Multidisciplinary Research and Development, 2*(3), 437–446.

Nganga, W. B., Ng'etich, K. O., Macharia, M. J., Kiboi, N. M., Adamtey, N., & Ngetich, K. F. (2020). Multi-influencing-factors' evaluation for organic-based soil fertility technologies outscaling in Upper Tana Catchment in Kenya. *Scientific African, 7*, e00231.

Odada, E.O. (2006). *Freshwater resources of Africa: Major issues and priorities*. Global Water News, No. 3. http://www.gwsp.org/downloads/GWSP_NL3_internet.pdf

Ogbonnaya, I., Ifediegwu, S. I., & Onwuka, O. S. (2020). Determining the occurrence of potential groundwater zones using integrated hydro-geomorphic parameters, GIS, and remote sensing in Enugu State, Southeastern Nigeria. *Sustainable Water Resources Management, 6*(39), 1–14. https://doi.org/10.1007/s40899-020-00397-5

Oh, H. J., Kim, Y. S., Choi, J. K., Park, E., & Lee, S. (2011). GIS mapping of regional probabilistic groundwater potential in the area of Pohang City, Korea. *Journal of Hydrology, 399*(3–4), 158–172. https://doi.org/10.1016/j.jhydrol.2010.12.027

Ostad-Ali-Askari, K., & Shayannejad, M. (2021). Quantity and quality modelling of groundwater to manage water resources in Isfahan—Borkhar Aquifer. *Environment, Development and Sustainability*. https://doi.org/10.1007/s10668-021-01323-1

Ostad-Ali-Askari, K., Shayannejad, M., & Ghorbanizadeh-Khorazi, H. (2017). Artificial neural network for modeling nitrate pollution of groundwater in marginal area of Zayandeh-Rood River, Isfahan, Iran. *KSCE Journal of Civil Engineering, 21*(1), 134–140. https://doi.org/10.1007/s12205-016-0572-8

Otezie, G. E. (1976). The hydrogeology of Northwestern Nigerian Basin. In C. A. Kogbe (Ed.), *Geology of Nigeria* (pp. 373–390). Elizabethan Pub.

Prabhu, M. V., & Venkateswaran, S. (2015). Delineation of artificial recharge zones using geospatial Techniq Naduues in Sarabanga sub basin Cauvery River, Tamil. *Aquatic Procedia, 4*, 1265–1274. https://doi.org/10.1016/j.aqpro.2015.02.165

Raju, R. S., Raju, G. S., & Rajasekhar, M. (2019). Identification of groundwater potential zones in Mandavi River basin, Andhra Pradesh, India using remote sensing, GIS and MIF techniques. *HydroResearch, 2*, 1–11. https://doi.org/10.1016/j.hydres.2019.09.001

Shaban, A., Khawlie, M., & Abdallah, C. (2006). Use of remote sensing and GIS to determine recharge potential zones: The case of Occidental Lebanon. *Hydrogeology Journal, 14*(4), 433–443. https://doi.org/10.1007/s10040-005-0437-6

Thapa, R., Gupta, S., Guin, S., & Kaur, H. (2017). Assessment of groundwater potential zones using multi-influencing factor (MIF) and GIS: A case study from Birbhum district, West Bengal. *Applied Water Science, 7*(7), 4117–4131. https://doi.org/10.1007/s13201-017-0571-z

Umar, I. U. (2000). An outline of the hydrogeology of the Sokoto-Rima basin in Nigeria. *First National Workshop on Applications of Isotope Techniques in Water Resources Development and Management.* Sokoto, Nigeria.

UNEP (2002). State of the environment and policy retrospective: 1972–2002. In: *Global environment outlook 3*: *Past, present and future retrospectives*.

Waikar, M. L., & Nilawar, A. P. (2014). Identification of groundwater potential zone using remote sensing and GIS technique. *International Journal of Innovative Research in Science, Engineering and Technology, 3*(5), 12163–12174.

WGS (1984). The World Geodetic Coordinate Systems.

Zealand, C. M., Burn, D. H., & Simonovic, S. P. (1999). Short term streamflow forecasting using artificial neural networks. *Journal of Hydrology, 214*(1–4), 32–48.